

THE SEPARATION OF OCEANIC TEMPERATURE FINESTRUCTURE AND INTERNAL MOTION

Thermistor data taken in the ocean with instrumentation systems such as the APL towed oceanographic chain show both high and low irregular variability — a manifestation of the finestructure of vertical temperature profiles. Making physically plausible assumptions about the nature of the fluid motion results in a data processing technique that permits temperature data to be separated into an undisturbed vertical profile and underlying fluid displacements. This technique is demonstrated on simulated and actual towed-thermistor-chain data and is shown to be superior to other methods that are based on interpolated isotherms or averaged profiles.

INTRODUCTION

Vertical temperature profiles taken in the ocean exhibit small-scale variations that make difficult the interpretation of temperature data in terms of fluid motion. In regions with small local temperature gradients, small fluid displacements result in small temperature variations, whereas in regions with large local gradients, small fluid displacements may result in disproportionately large temperature fluctuations.

The problem is illustrated most simply by considering the temperature measured at a fixed point in the oceanic thermocline. A typical vertical temperature profile consists of a series of irregular steps. These steps are composed of regions of relatively constant temperature called *layers* and regions of rapid temperature variations called *sheets*. Fluid motion causes the whole structure of sheets and layers to heave and subside past the fixed observation point, and the temperature time series data reflect this oscillation. A simplified example of this phenomenon is shown schematically in Fig. 1. Figure 1a illustrates a vertical temperature profile that consists of two relatively thick layers separated by a very thin sheet. If a sinusoidal wave were induced in a body of water having this profile, the interface would oscillate up and down with time as shown in Fig. 1b. A temperature sensor located at the fixed depth shown would alternate being in one layer or the other, with corresponding square-wave time-series response as shown in Fig. 1c. Clearly, the raw temperature data cannot be used to infer fluid motion directly. The apparent square-wave behavior of the temperature data is an example of finestructure contamination.

If the vertical temperature gradient in the ocean were uniform instead of irregular, the vertical displacement ζ of a fluid element would be proportional to the variation in temperature T according to the relation

$$\zeta = \left(\frac{\partial \bar{T}}{\partial z} \right)^{-1} (T - \bar{T}), \quad (1)$$

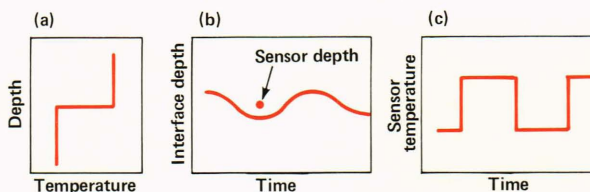


Figure 1 — Simplified example of finestructure contamination: (a) temperature profile showing two layers separated by a sheet; (b) sinusoidal oscillation of the interface; and (c) resulting temperature record.

where \bar{T} is the average temperature and z is depth. In a layered structure, however, such is clearly not the case. In fact, spectra and coherences of temperature fluctuations observed in this way in a layered sea may have little to do directly with the spectra and coherences of displacements. Similar fluctuations occur for measurements of temperature along a horizontal traverse.

The reasons for this ubiquitous finestructure in stably stratified regions are not yet clear. Such mechanisms as double-diffusive processes, intrusions, and internal wave breaking have been proposed as possible explanations for its existence.¹ However, this article is concerned only with the interpretation of temperature data in terms of fluid motion. In what follows, the models of finestructure contamination are first reviewed briefly. It is then shown that, by using the passive finestructure model and by making physically plausible assumptions about the character of the fluid motion, finestructure contamination can be greatly reduced. Referring to the simple example of Fig. 1, it is shown that there is a method for inputting only data like those shown in Fig. 1c and deriving data like those shown in both Figs. 1a and 1b. This result is achieved by separating temperature data into an undisturbed vertical temperature profile and underlying fluid displacements. The physical assumptions are incorporated into a displacement field action, and the separation is uniquely specified by

minimizing this action. This technique is demonstrated on simulated and actual towed thermistor-chain data, and its superiority over other methods is also shown.

MODELS OF FINESTRUCTURE CONTAMINATION

Phillips,² Reid,³ Garrett and Munk,⁴ McKean,⁵ and others⁶⁻⁸ model finestructure contamination in the following manner. The temperature field is given by

$$T(\vec{x}, t) = T_0 [z + \zeta(\vec{x}, t)]. \quad (2)$$

All of the small-vertical-scale irregularity is contained within the undisturbed temperature profile $T_0(z)$. Because no horizontal space or time variation is incorporated, this profile is referred to as “passive.” In addition, all the models assume that the displacement field is a linear internal wave field. Real oceanic finestructure should, of course, have a dependence on space and time that is not caused solely by the space-time variations of internal waves. However, it is assumed that any space or time dependence of $T_0(z)$ is so slight that it can be ignored. In fact, Garrett and Munk⁴ verify the assumption that the finestructure is indeed a sufficiently slowly varying function of space and time. They show that the finestructure contribution to spectra occurs at scales that are small compared with the persistence of the finestructure.

Figure 2 shows a model example of the effects of finestructure contamination on temperature frequency spectra. The particular model shown is that of Garrett and Munk,⁴ but the qualitative effects of finestructure are common to all the models. For a relatively low Cox number, C_1 (ratio of root mean square to mean temperature gradient), the finestructure softens the spectral break at the Brunt-Väisälä frequency N (the frequency at which a small, neutrally buoyant particle will oscillate when displaced from its equilibrium depth in a vertically varying field) and dominates the spectrum at higher frequencies. For a larger Cox number, C_2 , the break at N may be totally obscured and accompanied by a break in slope for frequencies less than N . There is general agreement that large Cox numbers are associated with high degrees of contamination. It has been shown by Phillips² and others that finestructure is responsible for a loss of vertical coherence in temperature even if the vertical motions causing the temperature fluctuations are perfectly correlated.

Although it is not a method of separation, one way of reducing finestructure contamination is to compute the depth of a single fixed temperature. This depth is known as an isothermal depth, and the locus of such isothermal depths is called an isotherm. In principle, exact isotherms have no finestructure contamination. However, any real data set allows only approximate isotherms to be calculated. The errors induced by these approximations limit their utility.

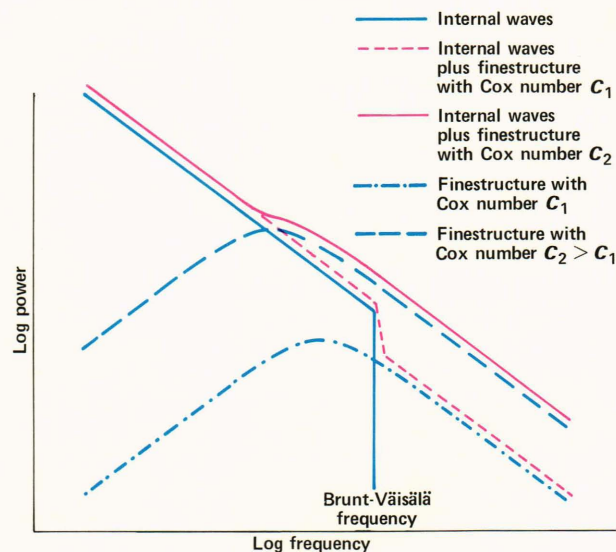


Figure 2 — Moored temperature frequency spectra for the Garrett and Munk⁴ model showing finestructure contamination. The model is shown for (a) internal waves only (no finestructure contamination), (b) low Cox number C_1 (ratio of root mean square to mean temperature gradient) resulting in low contamination, and (c) higher Cox number C_2 resulting in higher contamination.

One technique that has been demonstrated by Pinkel⁹ is to compute successive isotherms from a continuously profiling temperature sensor. The sensor is raised and lowered so that it always crosses a particular isotherm. However, it usually takes several seconds to complete a profiling cycle; hence, scales shorter than the profiling period are not attainable by this method.

Another technique that is applicable to moored or towed thermistor chains is to compute interpolated isotherms. The errors inherent in interpolating isotherms can be seen by the following considerations. Because of data rate limitations and limitations of relative sensor accuracy, any towed or moored thermistor array must have a finite number of sensors that are separated in the vertical dimension. Thus, isotherms must be interpolated between adjacent thermistors. However, temperature finestructure in the ocean causes variations that are often smaller than a given sensor spacing. The result is an interpolation error caused by finestructure contamination.

Figure 3 shows some isotherms simulated from the GM76 model,¹⁰ a specified temperature profile taken from one of the St. Croix experiment CTD (conductivity, temperature, depth sensor) casts,¹¹ and the resulting interpolated isotherms for a 2-meter sensor spacing. As should be expected, the interpolated isotherms agree well with the exact isotherms at depths over which there is little temperature variation. However, in regions where there are large variations, large interpolation errors result. Nonphysical spikes and steps that are not representative of fluid motion are typical of actual oceanographic interpolated isotherm data.

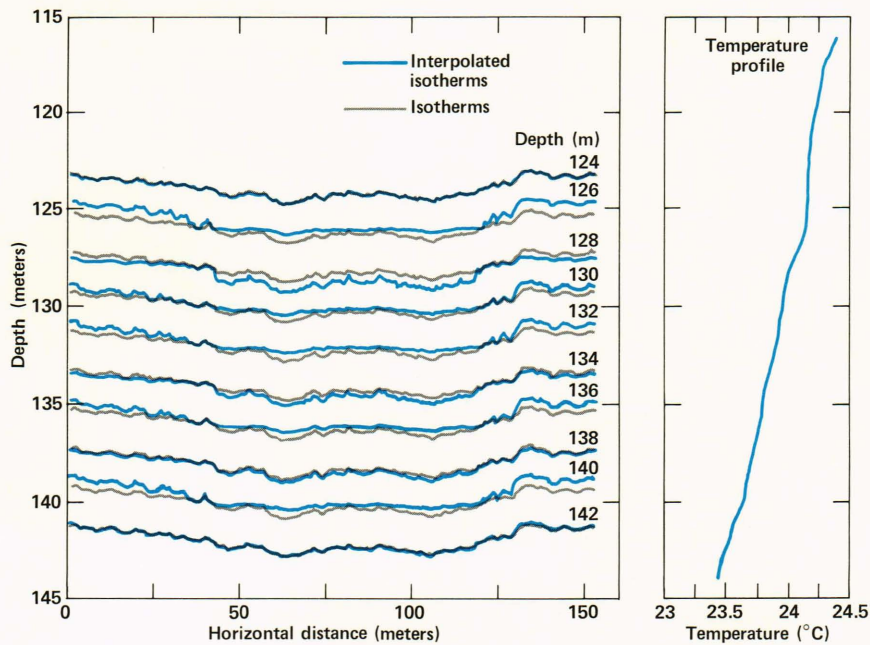


Figure 3 — Comparison of isotherms and interpolated isotherms for the temperature profile shown and simulated GM76 data.¹⁰ Isotherms are chosen so that their initial depths are 2 meters apart.

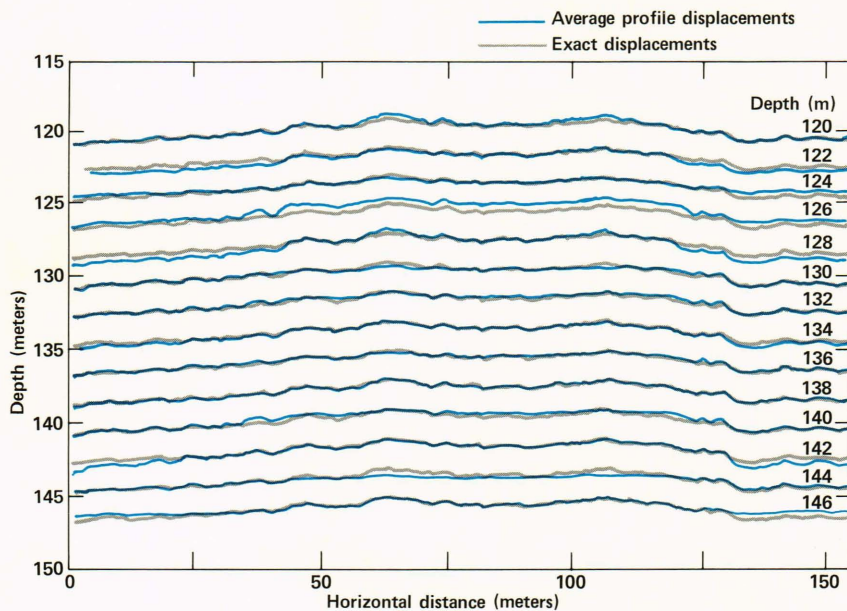


Figure 4 — Comparison of exact and average profile displacements for simulated GM76 data.

In addition to isotherms, another method that has been used in the past for computing displacements is to calculate an average profile and then compute displacements from this profile.¹² Unfortunately, the process of averaging tends to smooth out all the small-scale structure of the profiles. Since the profile varies smoothly, the irregularities of temperature data are transmitted to the resulting displacements. Figure 4 shows an example of this effect. The temperature data used to generate Fig. 2 are averaged over the horizontal, and the displacements calculated from this average profile are shown in Fig. 4 along with the exact specified displacements. The result shows large errors for regions where there are sharp variations in the undisturbed profile.

THE METHOD OF SEPARATION

It will now be shown that making physically plausible assumptions about the character of oceanic temperature variations leads to a well-defined method of separating temperature data into a finestructure component and a motion component. The first major assumption is that the passive finestructure model can be applied directly to real oceanic temperature-time series. Of course, any temperature field $T(\vec{x}, t)$ can be written as a displacement ζ of some profile. The problem is to find the undisturbed profile $T_0(z)$ for which the vertical displacements are relatively free from nonphysical irregularities. Any instantaneous profile at a point (from, say, a CTD cast)

will always be strained and advected by fluid motion and therefore would not represent a true undisturbed profile.

A condition is required in order to specify uniquely the undisturbed temperature profile and the corresponding displacement field. A natural condition that is consistent with the models of finestructure contamination is that the displacement field be a linear internal wavefield. It is certainly true that there must be nonlinearities in the displacement field. However, it is generally believed that these nonlinearities are perturbative in nature so that, to a first approximation, we can assume linearity. With this assumption, the displacement field $\zeta(\vec{x}, t)$ satisfies the linear internal wave equation of motion. Given $T(\vec{x}, t)$, the equation of motion, and Eq. 2, it is theoretically possible — but in practice very difficult — to solve for $T_0(z)$ directly. However, there is an alternative formulation that facilitates solution. This alternative employs a quantity known as the *action* (the integral of energy over a time interval).

If we define the action, $S[\zeta]$, as

$$S[\zeta] = \int d^3x dt \left[\left(\frac{\partial}{\partial t} \nabla \zeta \right)^2 - N^2 \left(\nabla_h \zeta \right)^2 \right], \quad (3)$$

and require that the displacement field be such that $S[\zeta]$ is a minimum, then the linear internal wave equation follows. The technique of deriving hydrodynamic equations of motion from a principle of least action is well known and has been used by Whitham,¹³ Olbers,¹⁴ and others. Nonlinear effects can be easily incorporated into the action by the addition of perturbative terms. The action written in Eq. 3 is for the constant N case in the absence of mean shear.

We now state the first major theorem: given a temperature field $T(\vec{x}, t)$ and that there exist an undisturbed profile $T_0(z)$ and a linear internal wave displacement field $\zeta(\vec{x}, t)$ such that $T(\vec{x}, t) = T_0[z + \zeta(\vec{x}, t)]$, then $T_0(z)$ is given by the profile that minimizes the action S . The proof of this theorem is obvious: since ζ is required to be a minimum of S and for a fixed T , T_0 specifies ζ by means of the passive finestructure model, then T_0 must be such that S is a minimum.

This theorem is intuitively very appealing. By assigning the subsequent action with a correspondingly large value, the theorem recognizes that a wrong guess for the temperature profile would cause anomalies in the form of irregularities and high gradients for the displacement field. A better guess for the undisturbed profile would give a field ζ with reduced irregularity and gradients and with a resulting smaller action. The best profile would be the true undisturbed one that contained all the structure of sheets and layers. The corresponding displacement field would be smoothly varying and the action would be a minimum.

The theorem specifies a unique method of separating finestructure effects from those of fluid motion if

the temperature field is completely known. Unfortunately, such four-dimensional data are difficult to obtain. Such constraints, therefore, limit its practical utility. What would be more useful would be a method that could be applied to two-dimensional data such as those from a towed or moored thermistor chain.

Consider a two-dimensional temperature field, $T(x, z)$, that is specified in only a vertical dimension and in one horizontal dimension. Such a field could be completely measured by a thermistor chain with infinite sensor density and towed at infinite speed. Assuming passive finestructure, there is a corresponding displacement field specified in two dimensions $\zeta(x, z)$. There does not exist an equation of motion for this two-dimensional field because the motion is in four dimensions.

However, there does exist a quantity $S_2[\zeta(x, z)]$, which may also be referred to in physical terms as an action, that completely specifies the probability space of the two-dimensional field $\zeta(x, z)$.¹⁵ The subscript 2 is used to distinguish it as a two-dimensional probability action as opposed to the four-dimensional action $S[\zeta(\vec{x}, t)]$. Basically, $S_2[\zeta(x, z)]$ provides the probability weighting for the occurrence of a single realization $\zeta(x, z)$, and the most probable field configuration is given by its minimum.

We now state the second major theorem: given a two-dimensional temperature field $T(x, z)$ and given that there exists an undisturbed profile $T_0(z)$ and a two-dimensional displacement field $\zeta(x, z)$ such that $T(x, z) = T_0[z + \zeta(x, z)]$, then the most probable profile T_0 is that which minimizes the probability action $S[\zeta(x, z)]$. The proof of this theorem is also straightforward: since $S_2[\zeta]$ is required to be a minimum at the most probable ζ and, for a fixed T , T_0 specifies ζ by means of the passive finestructure model, the most probable T_0 must be such that $S_2[\zeta]$ is a minimum.

In order to apply the above theorem to a given temperature field $T(x, z)$, it is necessary to derive a specific form for the action $S_2[\zeta]$. First, we assume that $\zeta(x, z)$ can be represented as a homogeneous, Gaussian, random field. Gaussianity and horizontal homogeneity have been verified for long-wavelength oceanographic isothermal displacement data. Vertical symmetry has also been verified.¹⁶ If vertical scales are restricted to those smaller than the variation of the Brunt-Väisälä frequency profile, the assumption of vertical homogeneity is not unreasonable.

Since it is well known that the spectra are dominated by long wavelengths, one can also make an approximation that is accurate for long wavelengths. One then obtains an approximation to the action $S_2[\zeta]$ that is an effective action:

$$S_E[\zeta] = \int dx dz \left[\alpha \zeta^2 + \beta \left(\frac{\partial \zeta}{\partial x} \right)^2 + \gamma \left(\frac{\partial \zeta}{\partial z} \right)^2 \right]. \quad (4)$$

The appropriateness of the effective action to various vertical scales can be clarified by the following discussion. Let L be the scale variation for the average Brunt-Väisälä frequency profile (typically larger than a few hundred meters) and let h be an average width of a layer (typically of the order of meters). Internal wave displacements with vertical wavelengths $\lambda_z \gg h$ are not significantly affected by finestructure variations of the profile but, rather, by the large-scale variation L . On the other hand, a vertical data window much smaller than L can lead to a constant- N assumption that subsequently implies vertical homogeneity. Consequently, the effective action (Eq. 3) is appropriate to the choice of a vertical window size W_z of the order of tens of meters that is between h and L ; i.e., $h \ll W_z \ll L$. The spectrum for this window size is then dominated by the longest wavelengths in the window.

We now have a well-defined method for separating two-dimensional temperature data into an undisturbed profile and a vertical displacement field. Given $T(x, z)$, $T_0(z)$ is specified by the requirements that $T(x, z) = T_0[z + \zeta(x, z)]$ and that $S_E[\zeta]$ be a minimum. Note that the only assumptions used in deriving $S_E[\zeta]$ are those of Gaussian distribution, homogeneity, and the dominance of long wavelengths. It is not assumed that ζ is a linear internal wave.

The numerical implementation of this method is accomplished by means of nonlinear programming and optimization methods. The multiparameter minimization is carried out by starting with an initial guess for the profile. The particular initial guess is not important except to reduce computation time. The action is calculated for a few points near the guess, and the profile is updated to a point with a lower action. This procedure is repeated until the lowest action is obtained. There are many different methods for implementing this optimization, such as gradient, Newton, and simplex methods. Results using the modified Fletcher-Powell method¹⁷ are discussed in the next section.

DEMONSTRATIONS OF THE METHOD

The method of separation is now demonstrated for simulated and actual towed thermistor-chain data. The superiority of this technique over methods based on interpolated isotherms or averaged profiles is also shown. Three cases for which the method was demonstrated are discussed.

In the first case, a simulated displacement field and an undisturbed temperature profile are selected in order to determine if the method would reproduce the original displacement field and undisturbed profile. A data window is selected that extends 28 meters in the vertical and 150 meters in the horizontal. These are scales for which interpolated isotherm errors are significant. The data are sampled every 2 meters in the vertical and 0.6 meter in the horizontal. The displacement is chosen to be a vertically coherent sine wave with a wavelength of 19.2 meters and an amplitude of 1 meter. This kind of displacement field is characteristic of a thermistor chain that moves as a rigid body and is driven by surface-wave-induced motion of the towing ship. The temperature profile assumed to be the undisturbed profile is from a CTD cast taken during the St. Croix experiment.¹¹ The profile is sampled every 1 meter in the vertical. Using the passive finestructure model results in the temperature data shown in Fig. 5. The sine waves are now distorted by the nonlinear variations of the finestructure. The large amplitude temperature variations reflect sheets and the small amplitude variations reflect layers. The corresponding average-profile displacements are illustrated in Fig. 6, which shows large errors for regions where there are sharp variations in the undisturbed profile. In fact, the root mean square error is comparable to the error for interpolated isotherms: viz., 25.4 and 32.5 centimeters, respectively. The interpolated isotherms and exact isotherms are shown in Fig. 7.

An algorithm has been written that numerically realizes the separation method described above. The particular optimization method used to minimize the

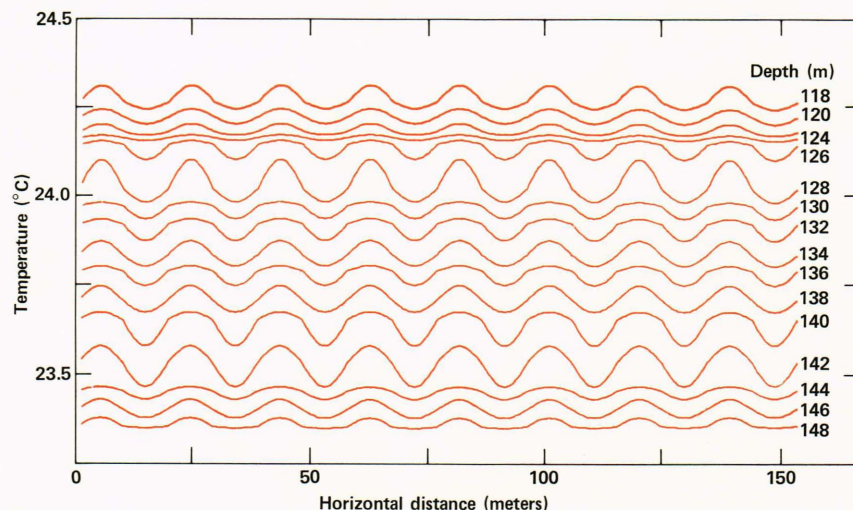


Figure 5 — Simulated thermistor-chain data for 2-meter spacing (chain motion case).

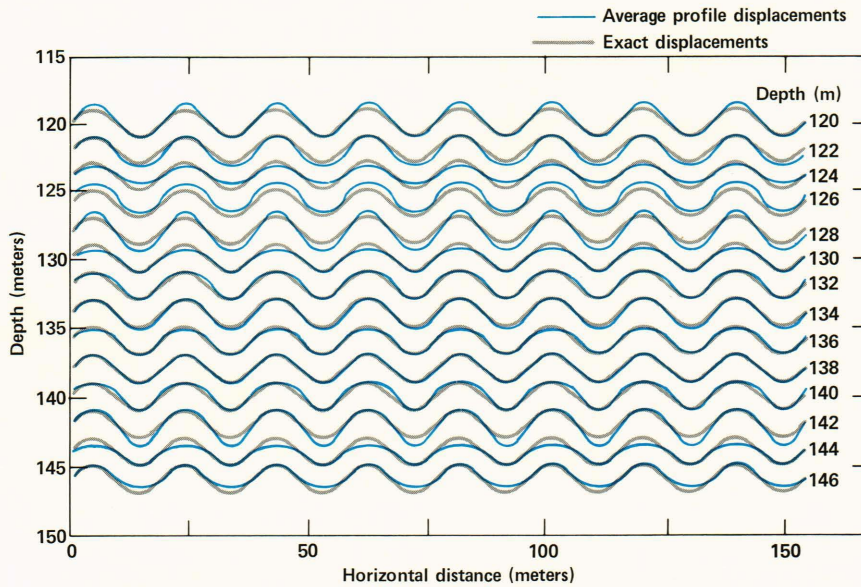


Figure 6 — Exact and average profile displacements for the chain motion case.

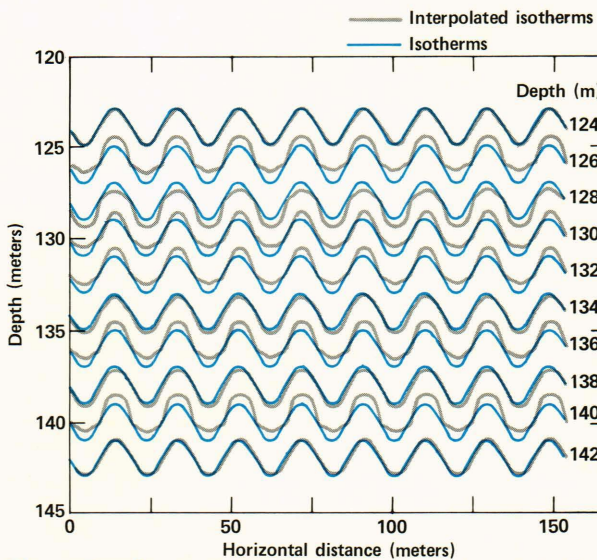


Figure 7 — Comparison of isotherms and interpolated isotherms for the chain motion case.

effective action is the modified Fletcher-Powell method. The initial guess is chosen to be the average profile. The optimization iteration is conducted, resulting in a calculated profile that shows little distinction between the exact and calculated profiles.

Figure 8 shows a comparison between the calculated displacements and the exact ones. The gray line represents displacements calculated by the algorithm while the black lines are the exact specified displacements. Except for the top and bottom traces, the calculated displacement is indistinguishable from the exact one. The root mean square error between exact and calculated displacements is 3.4 centimeters.

The second case in which the method is demonstrated uses simulated data wherein the displacement is a simulation of random data with a Garrett and Munk spectrum.⁴ This case is shown in order to dem-

	<i>Interpolated Isotherms</i>	<i>Average Profile Displacements</i>	<i>Separation Method</i>
Chain motion case	32.5	25.4	3.4
Garrett and Munk case	27.0	19.1	5.5

onstrate that the success of the method of separation is not specific to the sine wave case previously examined. The calculated profile resulting from the separation algorithm is once again indistinguishable from the exact specified profile. Table 1 is a comparison of the root mean square errors of these two cases, with the errors induced from the methods using interpolated isotherms or averaged profiles. The separation algorithm is a factor of 4 to 10 times better than the other methods.

The final case for consideration is that of actual oceanographic data. Figure 9 shows a sample of thermistor-chain data taken during the St. Croix experiment.^{8,11} (Figure 10 shows the R/V *Cape* towing a thermistor chain.) Because of thermistor failures, the vertical sampling is not uniform, and this fact must be taken into account. The sample of thermistor data clearly shows layers at 122, 138, and 142 meters and a sheet between 138 and 140 meters. When the method is applied to these temperature data, the resulting undisturbed profile shown in Fig.

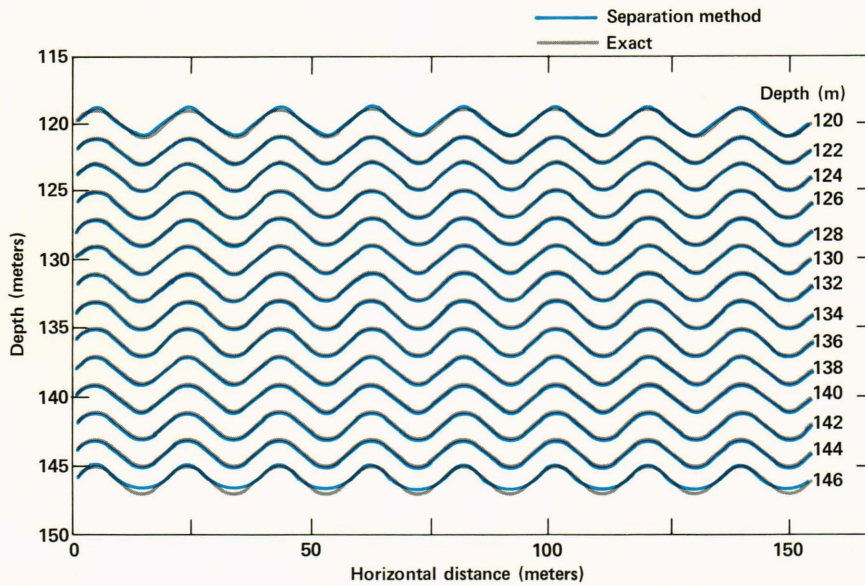


Figure 8 — Comparison of exact and separation method displacements (chain motion case).

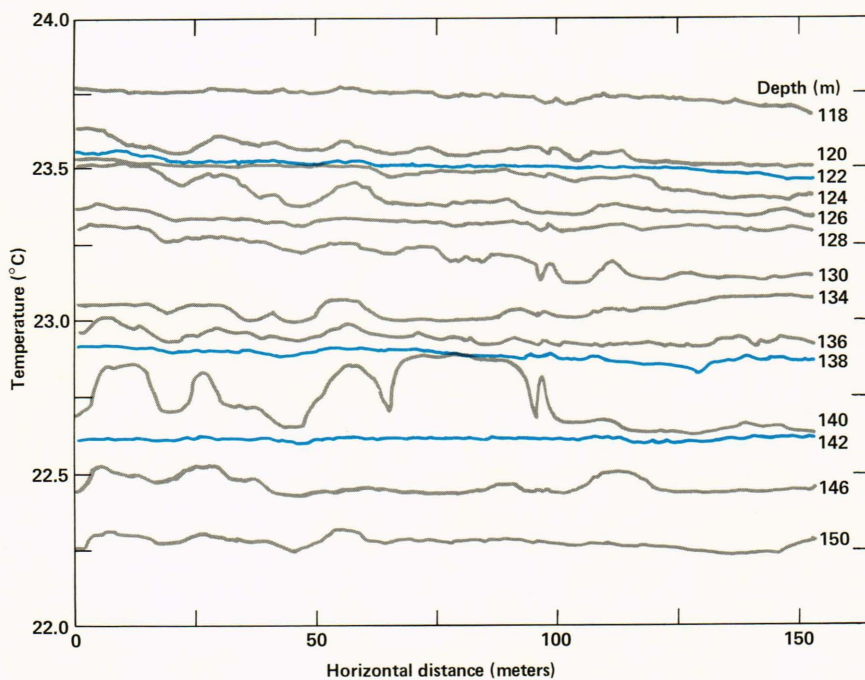


Figure 9 — St. Croix experiment thermistor-chain data. This sample of data shows regions of low temperature fluctuations (layers) at 122, 138, and 142 meters and a region of enhanced fluctuations (sheet) between 138 and 140 meters.

11 is obtained. In keeping with our qualitative observations on the temperature data, there is indeed a sheet between 138 and 140 meters and there are layers at 122, 138, and 142 meters. The corresponding displacement field shown in Fig. 12 has the relatively smooth variations expected of physical fluid motion.

Application of the other methods results in large irregularities in the average profile displacements in regions where there are large variations in the undisturbed profile. The displacements based on the separation method are much smoother and have a smaller root mean square displacement. There are also large irregularities in the interpolated isotherms for regions where there are large variations in the undisturbed profile. The processed data from the separation

method are much smoother and have smaller root mean square values.

COMMENTS AND CONCLUSIONS

In this article, a method that enables a separation between temperature finestructure and internal motions is introduced. The method is based on a passive finestructure model and a generalized principle of least action. Physically plausible assumptions about the fluid motion are incorporated into an action that, when minimized, yields an undisturbed temperature profile containing all the sheet and layer structure and a smoothly varying displacement field. The method is demonstrated on two-dimensional towed thermistor-chain data. Superiority over methods



Figure 10 — The R/V Cape towing a thermistor chain.

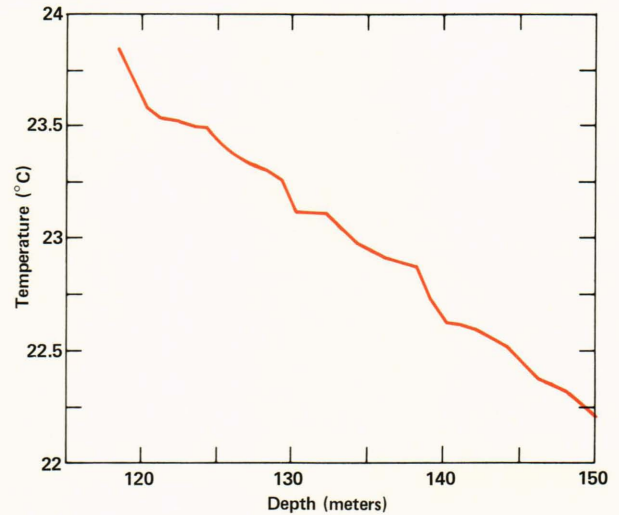


Figure 11 — Undisturbed temperature profile (from St. Croix thermistor-chain data) calculated using the separation method described in the text. In accordance with the qualitative observations of Fig. 9, the profile has low gradients (layers) at 122, 138, and 142 meters and a high gradient (sheet) between 138 and 140 meters.

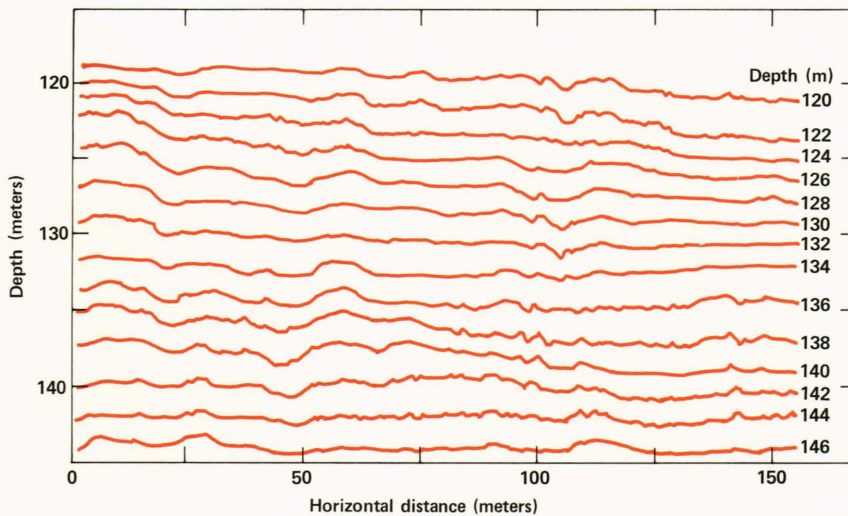


Figure 12 — Separation method displacement field from St. Croix thermistor-chain data.

based on isotherms or average profiles is also demonstrated. The method is robust because it was also successful for simulated cases that are not contained in the assumptions used to derive the action.

The major assumption of the separation method is that the undisturbed temperature profile $T_0(z)$ contains the entire sheet and layer structure that implicitly is coherent over the horizontal space (or time) aperture selected. In the real world, the undisturbed profile is expected to have space and time variations with finite coherence lengths. By taking a sufficiently small window, it is expected that any horizontal variation of T_0 with time is relatively negligible. What remains to be demonstrated is that T_0 varies on spatial scales much larger than the scales that are contaminated by finestructure.

REFERENCES and NOTES

- ¹See, for example, the collection of papers in the June 20, 1978 issue of *J. Geophys. Res.* **83** (1978); or the recent review, M. G. Briscoe and M. C. Gregg, "Internal Waves, Finestructure, Microstructure, and Mixing in the Ocean," *Rev. Geophys. Space Sci.* **17**, 1524-1548 (1979).
- ²O. M. Phillips, "On Spectra Measured in an Undulating Layered Medium," *J. Phys. Oceanogr.* **1**, 1-6 (1971).
- ³R. O. Reid, "A Special Case of Phillips' General Theory of Sampling Statistics for a Layered Medium," *J. Phys. Oceanogr.* **1**, 61-62 (1971).
- ⁴C. Garrett and W. Munk, "Internal Wave Spectra in the Presence of Fine-Structure," *J. Phys. Oceanogr.* **1**, 196-202 (1971).
- ⁵R. S. McKeen, "Interpretation of Internal Wave Measurements in the Presence of Fine-Structure," *J. Phys. Oceanogr.* **4**, 200-213 (1974).
- ⁶T. M. Joyce and Y. J. F. Desaubies, "Discrimination between Internal Waves and Temperature Finestructure," *J. Phys. Oceanogr.* **7**, 22-32 (1977).
- ⁷C. C. Eriksen, "Measurements and Models of Finestructure, Internal Gravity Waves, and Wave Breaking in the Deep Ocean," *J. Geophys. Res.* **83**, 2989-3009 (1978).
- ⁸M. W. Roth, "Response of the APL/JHU Chain to Motion and Finestructure," in L. Goodman, ed., *ONR Workshop on Horizontal*

- Variability, 1979* (in preparation).
- ⁹R. Pinkel, "Upper Ocean Internal Wave Observations from Flip," *J. Geophys. Res.* **80**, 3982-3910 (1975).
- ¹⁰C. Garrett and W. Munk, "Space-Time Scales of Internal Waves," *Geophys. Fluid Dyn.* **2**, 225-264 (1972); "Space-Time Scales of Internal Waves: A Progress Report," *J. Geophys. Res.* **80**, 291-297 (1975). The most recent version is referred to as GM76, which incorporates the observations of J. L. Cairnes and G. O. Williams, "Internal Wave Observations from a Midwater Float, 2," *J. Geophys. Res.* **81**, 1943-1950 (1976). See also T. H. Bell, Jr., *et al.*, "Internal Waves: Measurements of the Two-Dimensional Spectrum in Vertical-Horizontal Wave Number Space," *Science* **189**, 632-634 (1975); T. H. Bell, Jr., "Towed Thermistor Chain Measurements," *J. Geophys. Res.* **81**, 3709-3714 (1976); and the presentation of Y. J. F. Desaubies, "Analytical Representation of Internal Wave Spectra," *J. Phys. Oceanogr.* **6**, 976-981 (1976).
- ¹¹F. S. Billig, L. J. Crawford, and C. J. Gundersdorf, "Advanced Oceanographic Instrumentation Systems and Measurements," Paper No. 78-266, AIAA 16th Aerospace Sciences Meeting (1978).
- ¹²C. L. Johnson, C. S. Cox, and B. Gallagher, "The Separation of Wave-Induced and Intrusive Oceanic Finestructure," *J. Phys. Oceanogr.* **8**, 846-860 (1978).
- ¹³G. B. Whitham, *Linear and Nonlinear Waves*, John Wiley and Sons, New York (1974).
- ¹⁴G. J. Olbers, "Nonlinear Energy Transfer and the Energy Balance of the Internal Wave Field in the Deep Ocean," *J. Fluid Mech.* **74**, 375-399 (1976).
- ¹⁵A. S. Monin and A. M. Yaglom, *Statistical Fluid Mechanics*, MIT Press, Cambridge, Mass. (1971).
- ¹⁶M. C. Gregg, "A Comparison of Finestructure Spectra from the Main Thermocline," *J. Phys. Oceanogr.* **7**, 33-40 (1977); M. G. Briscoe, "Gaussianity of Internal Waves," *J. Geophys. Res.* **82**, 2117-2126 (1977); P. Muller, D. J. Olbers, and J. Willebrand, "The IWEX Spectrum," *J. Geophys. Res.* **83**, 479-500 (1978).
- ¹⁷R. Fletcher and M. J. D. Powell, "A Rapidly Convergent Descent Method for Minimization," *Comp. J.* **6**, 163-168 (1963); R. Fletcher, "A New Approach to Variable Metric Algorithms," *Comp. J.* **13**, 317-322 (1970).